Theor Chem Acc (2011) 130:1061–1069
DOI 10.1007/s00214-011-0984-y

REGULAR ARTICLE

Influence of polar groups on the wetting properties of vertically aligned multiwalled carbon nanotube surfaces

S. C. Ramos · A. O. Lobo · G. de Vasconcelos · E. F. Antunes · V. J. Trava-Airoldi · E. J. Corat

Received: 8 April 2011 / Accepted: 22 June 2011 / Published online: 15 July 2011

Abstract In this work, we have studied superhydrophilic and superhydrophobic transitions on the vertically aligned multiwalled carbon nanotube (VACNT) surfaces. As-grown, the VACNT surfaces were superhydrophobic. Pure oxygen plasma etching modified the VACNT surfaces to generate superhydrophilic behavior. Irradiating the superhydrophilic VACNT surfaces with a CO_2 laser (up to 50 kW cm^{-2}) restored the superhydrophobicity to a level that depended on the laser intensity. Contact angle and surface energy measurements by the sessile drop method were used to examine the VACNT surface wetting. X-ray photoelectron spectroscopy (XPS) showed heavy grafting of the oxygen groups onto the VACNT surfaces after oxygen plasma etching and their gradual removal, which also depended on the CO_2 laser intensity. These results show the great influence of polar groups on the wetting behavior, with a strong correlation between the polar part of the surface energy and the oxygen content on the VACNT surfaces. In addition, the CO_2 laser treatment created an interesting cage-like structure that may be responsible for the permanent superhydrophobic behavior observed on these samples.

Keywords Carbon nanotubes · Vertically aligned · Superhydrophobic · Superhydrophilic · Plasma etching · Laser irradiation

Dedicated to Professor Akira Imamura on the occasion of his 77th birthday and published as part of the Imamura Festschrift Issue.

S. C. Ramos (✉) · E. F. Antunes · V. J. Trava-Airoldi · E. J. Corat
Laboratorio Associado de Sensores e Materiais, Instituto Nacional de Pesquisas Espaciais, INPE, Avenida dos Astronautas, 1758, Jardim da Granja, São José dos Campos, SP 12227-010, Brazil
e-mail: sandra@las.inpe.br

S. C. Ramos
Departamento de Ciências, Universidade do Estado da Bahia, UNEB, Centro, S/N, Caetité, BA 46400-000, Brazil

A. O. Lobo
Laboratorio de Nanotecnologia Biomédica, Instituto de Pesquisa e Desenvolvimento, IP&D, Universidade do Vale do Paraíba, UniVaP, Avenida Shishima Hifumi, 2911, Urbanova, São José dos Campos, SP 12244-000, Brazil

G. de Vasconcelos
Instituto de Estudos Avançados, IEAv, Trevo Coronel Aviador José Albano do Amarante, 1, Putim, São José dos Campos, SP 12228-001, Brazil

E. F. Antunes
Instituto Tecnologico de Aeronáutica (ITA), Praça Marechal Eduardo Gomes 50, São José dos Campos, SP 12228-900, Brazil

1 Introduction

Carbon nanotubes (CNT) are promising materials for many potential applications because of their unique structures and properties [1, 2]. However, the hydrophobic and inert nature of the surface of as-grown nanotubes is unfavorable for some applications, as in microfluidic device [3, 4] or in contact with biological environments [5]. Therefore, it is necessary to adjust the surface, either chemically or physically, to comply with such applications. Based on the Cassie and Baxter model [6], some authors [7–9] discuss the effect of the nanotubes arrangement on superhydrophobic behavior, mainly its surface roughness on the micro and nano scales, compared with the gecko system [10]. This model is largely accepted to justify superhydrophobic

behavior of vertically aligned multiwalled carbon nanotube (VACNT) surfaces. The carbon nanotube wettability may be changed by employing chemical methods. As known, oxygen-containing functional groups attach onto nanotubes surfaces by oxidation treatment [11, 12] or acid treatment [13]. The wettability for polar liquids, such as water, improves significantly in this way, which leads to more reactive surfaces [14, 15]. Therefore, there is a need in the literature for more studies with the aim to better understand and control VACNT wettability.

This work advances considerably this aim. Two methods were used to modify the VACNT surfaces: oxygen plasma etching to graft efficiently polar groups onto the surfaces, and exposure to CO_2 laser irradiation to promote thermal desorption of the polar groups from the VACNT surfaces. Both methods were used to control wettability of VACNT surfaces: from superhydrophobic to superhydrophilic and back to superhydrophobic.

In addition, the CO_2 irradiation of the nanotube surfaces removed amorphous carbon and defects on the surface [16], improved their crystallinity [17] and promoted the appearance of a characteristic morphology, which resulted in a permanent superhydrophobic surface [18]. The good control of the surface wettability has also provided a better understanding of the VACNT wetting process: surface polarity can be used to control it. X-ray photoelectron spectroscopy (XPS), Raman spectroscopy and contact angle (CA) measurement examined the correlation between oxygen grafting and removal from the surface by monitoring the changes in polarity of VACNT, during both treatments. Images of scanning electron microscopy (SEM) with high resolution revealed the changes in surface morphology that could be responsible for variations in the wettability.

2 Materials and methods

A microwave plasma chamber built in our laboratory [19] produced the VACNT films in thin film form [20]. The substrates were 10 mm square Ti. A thin (10 nm) nickel layer, deposited by an e-beam evaporator, acted as catalyst. A pretreatment of the nickel layer formed nanoclusters from which the carbon nanotubes nucleate. The pretreatment duration was 300 s in N_2/H_2 (10/90 sccm) plasma at a substrate temperature of 690 °C. The nanotubes growth followed during 120 s at a temperature of 730 °C after pretreatment and the addition of CH_4 (14 sccm) to the gas mixture. The reactor pressure was 25 torr during the whole process. External heating with Ni–Cr resistance under the substrate was used to control the substrate temperature.

Pulsed DC discharge technique functionalized VACNT films by a quick grafting of polar functional groups onto nanotube surfaces. The power supply was an asymmetrical bipolar pulsed DC, operating between 20 and 70 kHz of pulse frequency. The discharge chamber operated at a working pressure of 80 mtorr at 1 sccm pure oxygen gas flow, peak voltage was −700 V and the duration of the treatment was 120 s. After this period, the functionalization stopped by turning off the power supply and evacuating the discharge chamber. The results of these procedures were the superhydrophilic surfaces of this polar-VACNT.

Applying CO_2 laser irradiation onto polar-VACNT surfaces controlled surfaces wettability. Laser treatment with CW CO_2 laser (Synrad Model J48) was performed in a N_2 atmosphere, with 50 W maximum output power and 70 kW cm^{-2} intensity. Two moving mirrors guided the laser beam that was focused in a controlled scan onto sample surfaces. Each sample was treated by 20 scans at a speed of 1,000 mm s^{-1} and resolution of 300 dpi. Only the intensity of CO_2 laser irradiation was varied for the following values 15, 25, 35 and 50 kW cm^{-2}.

A Krüss Easy Drop system utilizing the sessile drop method measured the CA at room temperature to evaluate the surface energy of as-grown, polar-VACNT and laser-treated VACNT films. Di-iodomethane, polyethlene glycol, glycerol and deionized water were used to estimate surface energy. The liquid drops placed onto the VACNT surfaces with a microsyringe were 2–4 μl. A video camera recorded and digitalized the drop image. The surface energy (γ) as well its dispersive (γ_d) and polar (γ_p) parts was calculated by Owens and Wendt Method [21], under experimental conditions supported by other authors [22, 23].

SEM images (Jeol JSM-5310 and JSM-6330F) were used to examine the morphological arrangement of the VACNT surfaces and high-resolution SEM images to evaluate the modification details in terms of surface morphology.

Raman spectroscopy is a valuable tool to characterize carbon-based nanostructures. In this work, Raman scattering spectroscopy (Renishaw 2000 system), with excitation by Ar^+-ion laser ($\lambda = 514.5$ nm) in backscattering geometry was applied to access structural changes onto the samples. The diamond peak at 1,332 cm^{-1} calibrated the Raman shift with all measurements controlled at 25 °C.

XPS measurements were used to analyze chemical modifications promoted by each treatment performed on the samples using the AlKα line with VG CLAMP hemispherical analyzer. The inelastic scattering background of the C1s and O1s electron core-level spectra was subtracted using Shirley's method. C1s at 284.5 eV was the reference for all binding energies (BE). The curve fitting and data analysis software Fityk 0.9.2 was used to assign the peaks locations and corresponding fitting of XPS spectra (http://www.unipress.waw.pl/fityk/).

3 Results and discussions

3.1 Surface energy of VACNT films

Figure 1 shows the surface morphology of the VACNT samples under study, as taken from SEM. Typical VACNT films grew roughly aligned upright from the substrate. A dense forest of aligned nanotubes formed (as shown in the inset of Fig. 1a) with their surface morphology determined by van der Waals interactions among the tube tips [24], as seen in Fig. 1a. Figure 1b–d show the different morphologies obtained for each surface treated VACNT after wetting with DI water. Figure 1b shows the morphology after wetting the as-grown VACNT, which is a quite typical morphology seen many wetting studies. The nanotubes bent and their tips joined forming irregular shapes on a micrometer scale. The accepted explanation for these irregular shapes is a partial wetting with bending caused by forces produced during slow water evaporation. The structure of Fig. 1b also gives support for the understanding of the VACNT superhydrophobicity based on the Cassie and Baxter model [6]. Figure 1c shows the typical morphology after wetting the polar-VACNT obtained by oxygen plasma etching. Some cracks showed up, but most of the surface was unchanged. The polar-VACNT became superhydrophilic and wet by DI water. Probably because of the complete wetting and water flow between the polar-VACNT, the forces induced by water flow and evaporation appear only on a larger scale, with the nanotubes bending occurring only at the crack limits. A different characteristic wetting of the VACNT surfaces was observed after CO_2 laser irradiation at 50 kW cm^{-2}. Figure 1d shows that the total alignment of VACNT remained unchanged. Indeed, the surface became again superhydrophobic, but instead of a simple recovery of the superhydrophobicity of the as-grown samples, the comparison of Fig. 1d with b shows that the latter became unwettable. In Fig. 1d, there is no tube bending because of wetting and evaporation processes.

Figure 2 shows typical higher resolution SEM images of the VACNT surfaces under study. Figure 2a shows that the

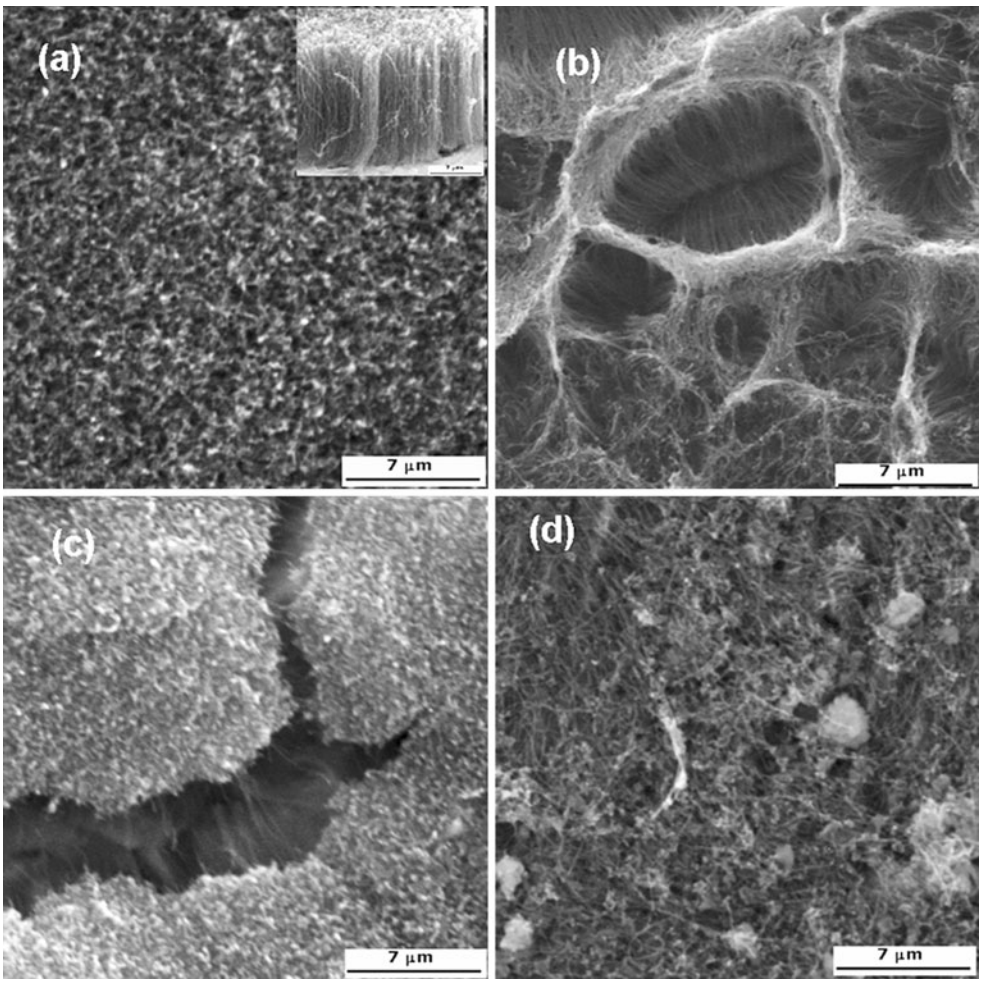

Fig. 1 SEM image of VACNT grown on Ti substrate: **a** surface and cross-section (*inset*) of as-grown VACNT. The effect of deionized water wetting on VACNT surface morphology: **b** as-grown VACNT, **c** polar-VACNT and **d** CO_2 laser-treated VACNT (at 50 kW cm^{-2})

surface as-grown samples have entangled arrangements not only with the tip tops of the VACNT but also with extended regions of their lateral surface. The surface attacked by the oxygen plasma is given in Fig. 2b. Clearly, the same entangled arrangements persist, but the nanotubes walls were damaged severely. The CO_2 laser treatment promoted evaporation of the tube tips. As shown in Fig. 2c, the parts of the nanotubes previously damaged by the oxygen plasma treatment almost completely evaporated when CO_2 laser irradiation at 50 kW cm^{-2} was applied to them. As a result of the tube tips evaporation, the entangled arrangements and the alignment of the CNTs were clearly seen. In addition, many nanotubes fused together at their tips forming cage-like structures homogeneously spread all over of the surface.

The wettability study of the VACNT surfaces performed by CA measurements, using the liquids cited above, allowed surface energy calculation by the Owens and Wendt method [21]. A complete description of these measurements should be found elsewhere [25]. Table 1 summarizes the values achieved for the surface energy (γ) and its polar (γ^p) and dispersive (γ^d) parts.

The surface energy values for as-grown VACNT were 50.5 mJ m^{-2}, with 48.7 and 1.8 mJ m^{-2} for its dispersive and polar parts, respectively. Remarkably, there is a huge increase in the polar part of the surface energy after the oxygen plasma treatment and this is the main reason for describing it as polar-VACNT. These measurements show clearly that the polar groups attached by the O_2 plasma efficiently changed polar part of surface energy due to chemisorptions of oxygen at reactive centers on the surface, which are formed during oxygen ions bombardment. This change on the polar part of the surface energy is responsible for the change from a superhydrophobic to a superhydrophilic character. CO_2 laser irradiation at 15, 25, 35 and 50 kW cm^{-2} has shown a gradual decrease in the polar part of surface energy, restoring the original value of the as-grown VACNT and, also the superhydrophobic character. These measurements proved that oxygen plasma etching causes effective change of the VACNT surface energy and that CO_2 laser treatment can restore it.

Notice that the superhydrophobic behavior after CO_2 laser treatment is not the same as in as-grown samples, even though their surface energies are similar. SEM images in Fig. 1a, d show this clearly. Slight increases of CA for wetting measurements are also indicative of these differences. Most important of all is the observation after long-term wetting experiments. The as-grown samples show a large CA at first, but the CA decreases after some minutes of being wet, pointing to the instability of its superhydrophobic behavior. The CA of CO_2 laser-treated samples did not

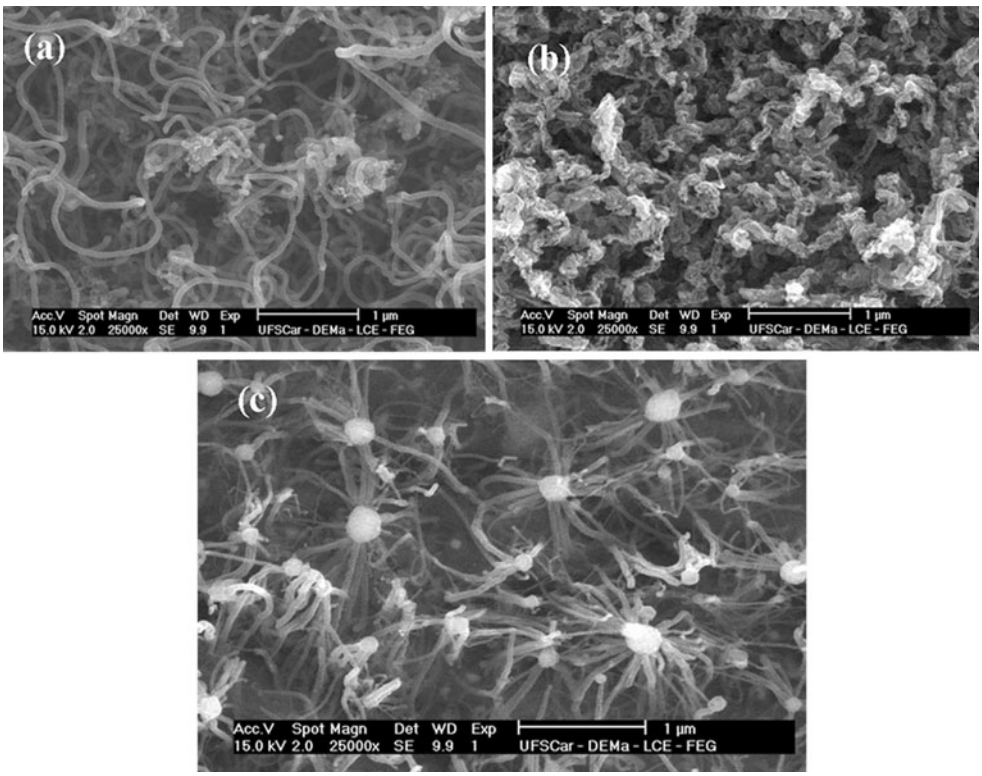

Fig. 2 High-resolution SEM images of the tube tips taken from: **a** as-grown VACNT, **b** polar-VACNT and **c** after CO_2 laser treatment at 50 kW cm^{-2}

Table 1 Surface energy (γ), dispersive (γ^d) and polar (γ^P) components from Owens and Wendt plot for polar-VACNT samples treated by CO_2 laser irradiation

CO_2 laser irradiation (kW cm^{-2})	γ (mJ m^{-2}) O_2 plasma etching	γ^d (mJ m^{-2}) O_2 plasma etching	γ^p (mJ m^{-2}) O_2 plasma etching
0	64.7	24.7	40
15	50.7	44.9	5.8
25	52.3	44.5	7.8
35	50.1	46.5	3.6
50	50.9	49.2	1.7

change even after several days of being wet, showing a permanent superhydrophobic behavior.

3.2 Raman spectra

Figure 3 shows first-order Raman scattering spectra of VACNT films for the as-grown VACNT (Fig. 3a), polar-VACNT (Fig. 3b), and CO_2 laser-treated VACNT at 35 kW cm^{-2} (Fig. 3c) and 50 kW cm^{-2} (Fig. 3d). The spectrum deconvolution in Fig. 3a, c, d was performed using Lorentzian shapes for the D and G bands, and Gaussian shape for the D' band, as pointed by the other authors [26]. For the spectrum deconvolution in Fig. 3b it was also necessary to include the Gaussian peak at 1,525 cm^{-1} in the fitting procedure. This band already appeared before for heavily functionalized carbon nanotubes [27]. In spite of this new band, whose origin is the polar groups grafting onto CNT surfaces, the following analysis was used to evaluate the changes in the D and G bands.

The changes of the *D* band can be used to explore structural modifications of the nanotube walls [28] owing to introduction of defects and attaching different chemical species [29]. Also, the D' band carries information about disorder in the sp^2 lattice [30]. Based on the fitting parameters, Table 2 summarizes the *full width at half-maximum* (*FWHM*) and the ratio of the integrated areas under the D and G bands (I_D/I_G).

The integrated intensity ratio of the D and G peaks (I_D/I_G) is often indicative of the level of chemical

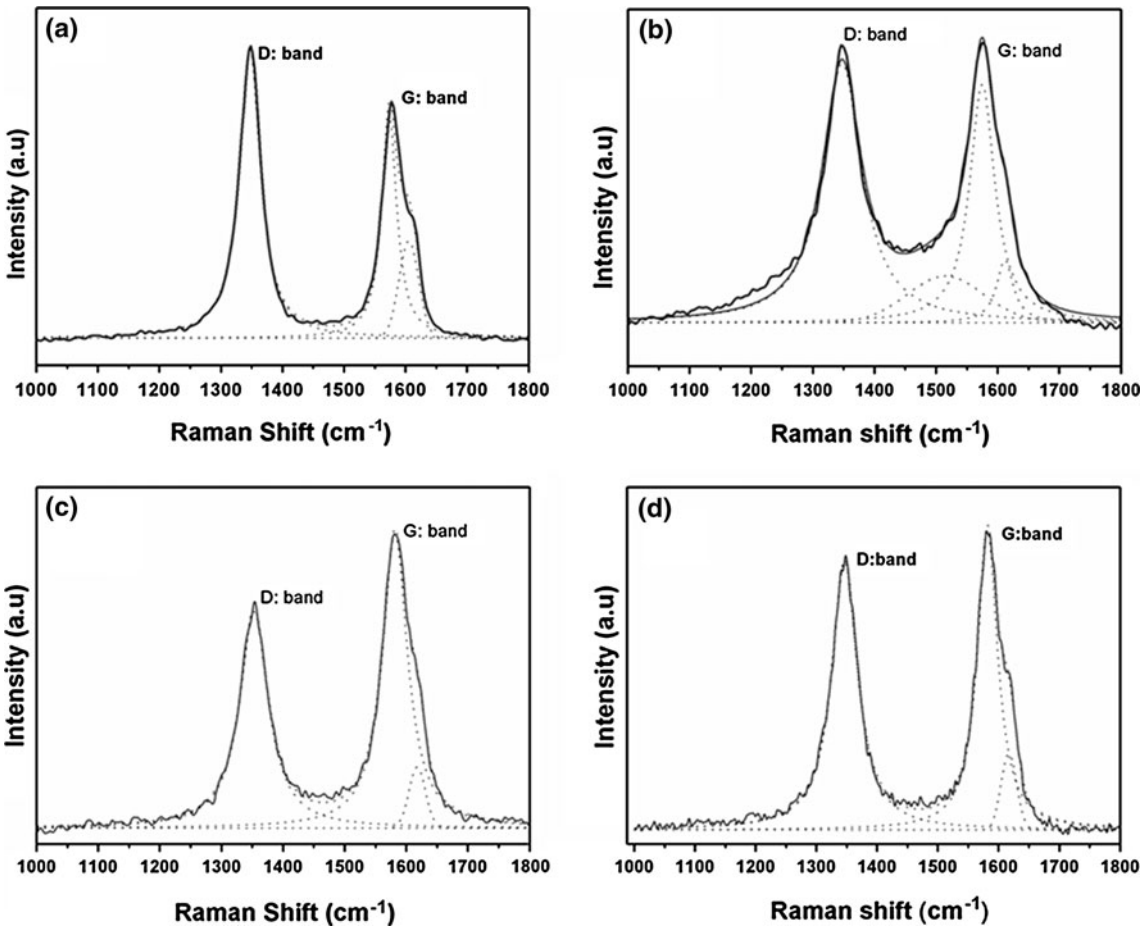

Fig. 3 Deconvolution of *D* and *G bands* for the VACNT under study: **a** as-grown VACNT, **b** polar-VACNT and after CO_2 laser irradiation on the polar-VACNT surface: **c** at 35 kW cm^{-2} and **d** at 50 kW cm^{-2}

Table 2 Gaussian and Lorentzian fitting results of Raman spectra (514.5 nm)

Sample under study	D band position (cm^{-1})	G band position (cm^{-1})	I_D/I_G	FWHM (D)	FWHM (G)
As-grown	1,348.4 ± 1.3	1,577.8 ± 2.2	1.6	42.0 ± 2.3	35.8 ± 2.1
O_2 plasma etching	1,350.5 ± 1.5	1,580.2 ± 2.5	1.7	91.2 ± 4.8	44.5 ± 3.3
O_2 plasma etching and CO_2 laser at 35 kW cm^{-2}	1,346 ± 2.8	1,578.2 ± 2.0	0.9	55.2 ± 1.3	46.03 ± 1.8
O_2 plasma etching and CO_2 laser at 50 kW cm^{-2}	1,345 ± 1.4	1,579.4 ± 1.2	1.0	49.3 ± 3.2	38 ± 3.8

functionalization or defect density of the CNT surfaces [29]. However, this ratio remained almost unchanged between the as-grown VACNT surfaces and their polar parts. This was due to the decreasing in D band intensity that occurs simultaneously with its broadening as well as the G band broadening. If both these spectra show similar I_D/I_G ratios, it could suggest a similar quantity of structural defects for as-grown and polar-VACNT. However, the comparison of Fig. 2a, b clearly shows that this is not the case. The D band broadening (FWHM), which increased from 42.0 to 91.2 cm^{-1}, was the most useful parameter to show that oxygen plasma treatment was effective for structure modification. In accordance with Dorai et al. [31] and the other studies [32–34] it is reasonable to assume that the reaction of atomic oxygen with high energy laser radiation breaks some of the C–C bonds of the carbon chain and leads to attachment of carboxyl groups that improve the wettability of the VACNT films by changing their polarity.

The CO_2 laser irradiation allowed reestablishment of VACNT characteristics by improving its crystallinity and by evaporating chemical species attached on its surface. This can be verified from analysis of the Raman spectra of the VACNT films taken after 35 and 50 kW cm^{-2} laser irradiation was applied to the polar VACNT surfaces, respectively, as seen in Fig. 3c, d and Table 2. By this treatment, I_D/I_G ratio decreased significantly, which is probably correlated with a drop in defect density [29, 30]. Changing of the intensity ratio of these peaks proved that structural defects originally present on the as-grown VACNT as well on the ones treated by oxygen plasma were gradually healed as the annealing laser power increased. This treatment also leads in a narrowing of the bands (I_D, I_G) for the samples previously treated by O_2 plasma to a level similar to the as-grown samples.

Raman spectra and wettability measurements showed that oxygen plasma etching and CO_2 laser irradiation in fact control wetting behavior by (i) the grafting of chemical species onto the surface and by (ii) evaporating the damaged surface nanotube tips that reduces the defect density. The overall observation suggested that the polar groups grafting, which considerably broadens the Raman bands, transforms the superhydrophobic as-grown samples back into superhydrophilic ones. CO_2 laser treatment removes the grafted polar groups, which narrows the Raman band linewidths close to the original values found for the Raman bands of the as-grown sample, and transforms the samples back to superhydrophobic. This analysis argues that the treated samples by CO_2 laser may be more superhydrophobic than the as-grown ones because they have a smaller defect density, as observed by the smaller I_D/I_G ratio.

3.3 XPS analysis

The XPS analyses are fundamental to uncover surface chemical composition. Figure 4 shows the C1s fitted photoemission spectra recorded for as-grown VACNT, polar-VACNT and after CO_2 laser treatment. The C1s curve of the as-grown VACNT (Fig. 4a) was deconvoluted into six peaks at 284.7, 285.5, 286.6, 287.5, 289.2 and 291.3 eV. The peaks correspond to aliphatic carbons (with C–C single bonds), carbon atoms with C–O, C–O–C or C–OH single bonds [33, 35], carbon atoms with C=O double bonds, and with carbon atoms with the COO^- carboxylate bonds, respectively. The last one at 291.3 eV is used to assign for the shake-up peak (π–π^* transitions) [36].

After exposing the samples to plasma etching, the C1s curve was also, deconvoluted into six peaks at 284.8, 285.9, 286.6, 287.9, 289.4, and 291.6 eV. The main peaks at 286.6, 287.9, 289.4 eV have shown a significant increase in area. This infers that strong C and O bonds formations [37, 38], mainly carboxyl groups that are situated at the ends of the tubes. In addition, the peaks around 284.9 and 285.9 eV showed and upshift. The change in area of this spectrum agrees with the information from the Raman spectra, but further proves that oxygen-based groups formed during the functionalization.

XPS analysis also further evaluated the effects of CO_2 laser irradiation on the polar-VACNT surfaces. The C1s spectrum deconvolution (Fig. 4c) on the samples irradiated by laser at 50 kW cm^{-2} showed a restoration to the spectrum of the as-grown VACNT (Fig. 4a). In this case, the C1s deconvolution presents peaks at 284.8, 285.7, 286.6, 287.8, 289.7, and 291.5 eV. This pointed out that laser heating of functionalized nanotubes in a N_2 atmosphere removed the carboxyl groups attached on them and restored the nanotube surface energy. This is also consistent with Raman data which suggested that functional groups were removed after applying CO_2 laser irradiation.

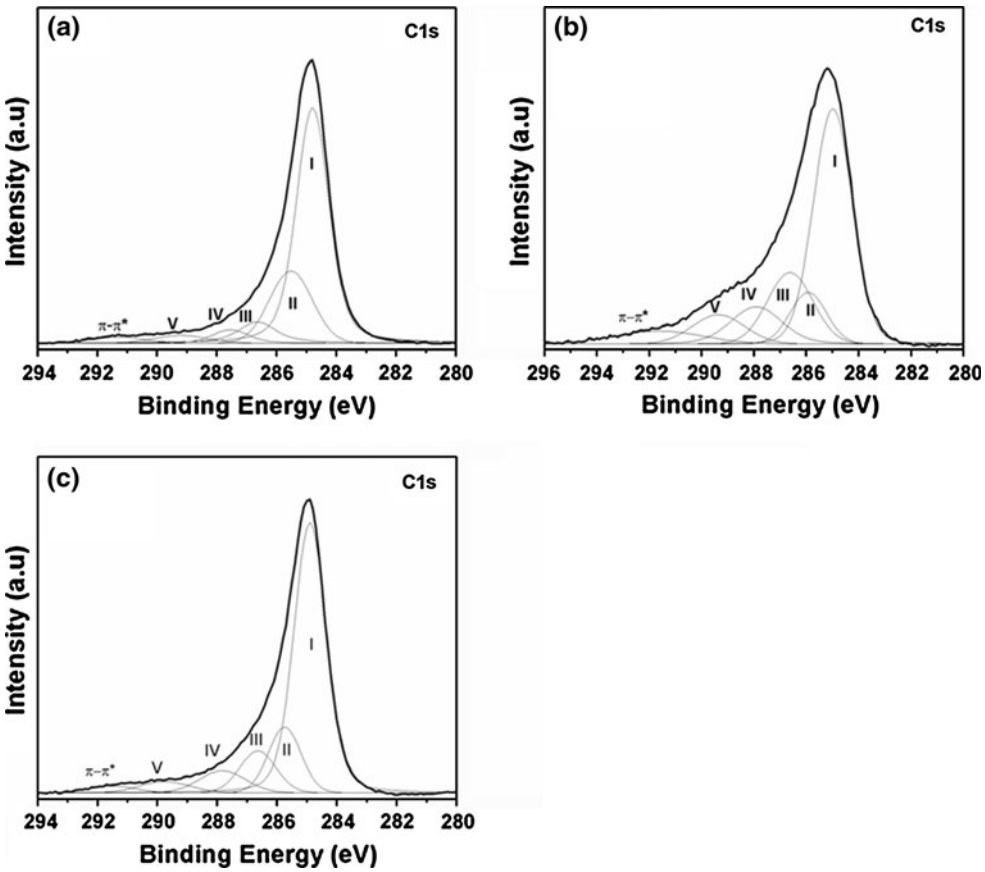

Fig. 4 XPS C1s deconvoluted peaks of **a** as-grown VACNT, **b** polar-VACNT and **c** polar-VACNT treated with CO_2 laser irradiation at 50 kW cm^{-2}

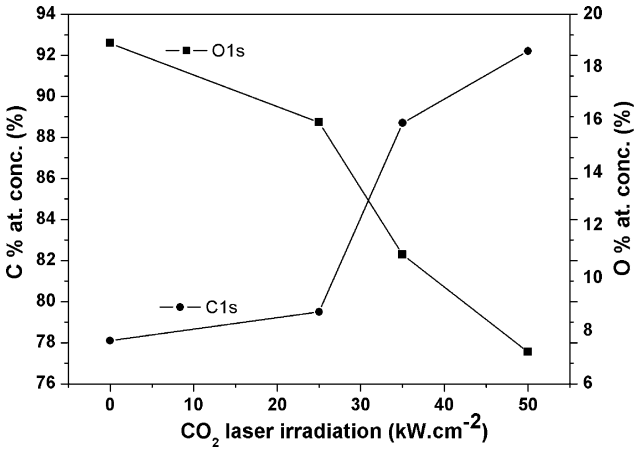

Fig. 5 C and O (at%) as a function of CO_2 laser irradiance on the polar-VACNT

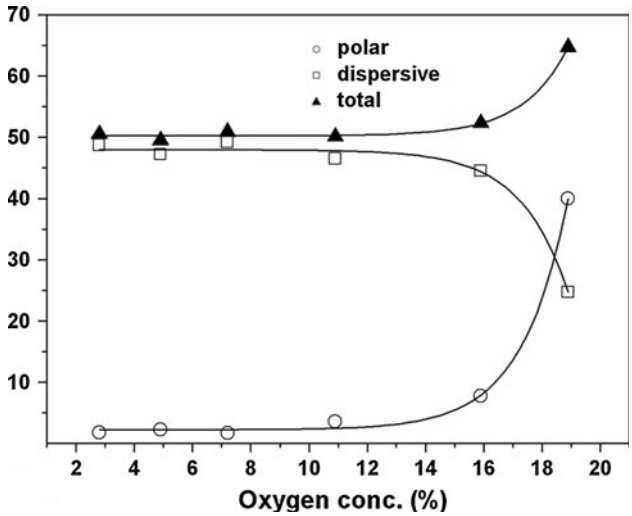

Fig. 6 Correlation between surface energies as a function of oxygen percentages on the samples surface analyzed

Indeed, the oxygen plasma technique promotes a heavy grafting of oxygen species onto surfaces. The percentages of carbon and oxygen of samples surface, as measured from XPS analysis, varied form 97.2 and 2.8%, on as-grown samples to 78.1 and 18.9%, after oxygen plasma etching. The CO_2 laser technique effectively removes the grafted oxygen species from the surface. Figure 5 shows total carbon and oxygen percentage onto surface as function of CO_2 laser irradiation on the polar-VACNT surface. After CO_2 laser treatment at 25, 35 and 50 kW cm^{-2} onto polar surface, the oxygen percentage was 15.9, 10.9 and 7.2%, respectively. The increase in C1s was also noticeable as function of CO_2 laser treatment. It increased from 78.1 to 79.5, and 88.7 and 92.2% as function of CO_2 laser irradiance.

Figure 6 shows a further correlation by plotting the surface energies seen in Table 1 as a function of percentage

of oxygen on corresponding sample surface. It shows three plots, one for the total surface energy, one for its dispersive part and one for its polar part. Total surface energy is nearly constant but increases for the largest oxygen coverage. Dispersive part decreases slightly with oxygen coverage. The polar part varied impressively, fitting neatly ($R = 0.9984$) to an exponential growth dependence on the oxygen coverage. The Fig. 6 makes clear that surface energy of the VACNT and, thus, its wetting behavior correlated with the coverage of polar groups on the surface. Some studies have already shown some variation onto surface energy by various methods for VACNT surface functionalization but none have shown such a huge variation and such a precise wetting control. The reason it was obtained here was the very effective functionalization resulted from the pure O_2 plasma etching. It grafted 18.9% oxygen on VACNT surface, while most results in literature showed only up to 14.4% after oxidized for 24 h in nitric acid [13].

Even though the surface coverage with polar groups can explain the overall wetting behavior, it remains unexplained the remarkable difference between the two superhydrophobic behaviors, of the as-grown VACNT and the CO_2 laser-treated one. Both have similar C1S XPS spectra. The overall analysis shown in this work points out two great differences that may contribute for the permanent superhydrophobic behavior of the CO_2 laser-treated samples. The first one is the higher crystalline quality as shown by the Raman spectroscopy. The second one is the surface's morphological arrangements as shown in the higher resolution SEM of Fig. 2c. The cage-like structure is very interesting because it may prevent the VACNT bending under wetting. Also, the air encaged on it may contribute for the nonwetting properties, as explained by a Cassie and Baxter model. This cage-like structure was already shown in nature to be superhydrophobic [39].

4 Conclusions

Wettability of the VACNT films significantly increases after oxygen plasma etching. This characteristic is because of the polar groups attached onto nanotube surfaces. CO_2 laser irradiation converted superhydrophilic surface back to superhydrophobic. This conversion, impelled by CO_2 laser irradiation, was because of the evaporating parts of the VACNT containing oxygen polar groups. Raman spectra and XPS analyzes allowed the study of chemical changes on the surface. Raman spectra shows that CO_2 laser treatment gives VACNT a better crystalline quality, and XPS analysis directly correlate the oxygen content with the polar part of the surface energy.

All results corroborated that polar groups and defects onto surface are decisive on the wetting characteristics of VACNT.

Of particular interest is the permanent superhydrophobic behavior achieved after CO_2 laser treatment. The higher crystalline quality suggested some influence in this behavior. However, the surface morphology detected, showing a cage-like structure, point out as the main reason for the effect. The cage-like structure itself may prevent VACNT bending under wetting, and the air encaged between the nanotubes may prevent wetting.

Acknowledgments This work was supported by FAPESB (720/2009) and FAPESP (07/00013-4, 06/03525-3 and 2008/11642-5) and UNEB. Special thanks to Maria Lucia Brison (LAS/INPE) by the SEM images, and Marcelo E. H. Maia da Costa (PUC/Rio) by XPS spectra.

References

1. Baughman RH, Zakhidov AA, Heer WA (2002) Carbon nanotubes the route toward applications. Science 297:787–792
2. Kouklin NA, Kim WE, Lazareck AD, Xu JM (2005) Carbon nanotube probes for single-cell experimentation and assays. Appl Phys Lett 87:173901–173903
3. Fu Q, Liu J (2005) Integrated single-walled carbon nanotube/microfluidic devices for the study of the sensing mechanism of nanotube sensors. J Phys Chem B 109:13406–13408
4. Ko H, Peleshanko S, Tsukruk VV (2004) Combing and bending of carbon nanotube arrays with confined microfluidic flow on patterned surfaces. J Phys Chem B 108:4385–4393
5. Lobo AO, Corat MAF, Antunes EF, Palma MBS, Pacheco-Soares C, Garcia EE, Corat EJ (2010) An evaluation of cell proliferation and adhesion on vertically-aligned multi-walled carbon nanotube films. Carbon 48:245–254
6. Cassie ABD, Baxter S (1944) Wettability of porous surfaces. Trans Faraday Soc 40:546–551
7. Oner D, McCarthy TJ (2000) Ultrahydrophobic surfaces effects of topography length scale on wettability. Langmuir 16:7777–7782
8. Lau KS, Bico J, Teo KB, Chhowalla M, Amaratunga GAJ, Milne WI et al (2003) Superhydrophobic carbon nanotube forests. Nano Lett 3:1701–1705
9. Hong YC, Uhm HS (2006) Superhydrophobicity of a material made from multiwalled carbon nanotubes. Appl Phys Lett 88:244101–244104
10. Ge L, Sethi S, Ci L, Ajayan PM, Dhinojwala A (2008) Carbon nanotube-based synthetic gecko tapes. Nano Lett 8:822–825
11. Ajayan P, Ebbesen W, Ichihashi T, Iijima S, Tanigaki K, Hiuria H (1993) Opening carbon nanotubes with oxygen and implications for filling. Nature 362:522–525
12. Kim Y, Lee D, Oh Y, Choi J, Baik S (2006) The effects of acid treatment methods on the diameter dependent length separation of single walled carbon nanotubes. Synt Met 156:999–1003
13. Lakshminarayanan PV, Toghiani H, Pittman CU (2004) Nitric acid oxidation of vapor grown carbon nanofibers. Carbon 42:2433–2442
14. Sun T, Wang G, Liu H, Feng L, Jiang L, Zhu D (2003) Control over the wettability of an aligned carbon nanotube film. J Am Chem Soc 125:14996–14997

15. Kakad BA, Pillai VK (2008) Tuning the wetting properties of multiwalled carbon nanotubes by surface functionalization. J Phys Chem C 112:3183–3186
16. Bai X, Dan L, Du D, Zhang H, Chen L, Ji L (2002) Laser irradiation for purification of aligned carbon nanotube films. Carbon 42:2125–2127
17. Cheong FC, Lim KY, Sow CH, Lin J, Ong CK (2003) Large area patterned arrays of aligned carbon nanotubes by means of laser trimming. Nanotechnology 14:433–437
18. Ramos SC, Vasconcelos G, Antunes EF, Lobo AO, Trava-Airoldi VJ, Corat EJ (2010) CO_2 laser treatment for stabilization of the superhydrophobicity of carbon nanotube surfaces. J Vac Sci Technol B 28:1153–1158
19. Antunes EF, Lobo AO, Corat EJ, Trava-Airoldi VJ, Martin AA, Veríssimo C (2006) Comparative study of first- and second-order Raman spectra of MWCNT at visible and infrared laser excitation. Carbon 44:2202–2211
20. Choi YC, Shin YM, Lim SC, Bae DJ, Lee YH, Lee BS, Chung D (2000) Effect of surface morphology of Ni thin film on the growth of aligned carbon nanotubes by microwave plasma-enhanced chemical vapor deposition. J Appl Phys 88:4898–4903
21. Owens DK, Wendt RC (1969) Estimation of the surface free energy of polymers. J Appl Polym 13:1741–1969
22. Yu MF, Lourie O, Dyer MJ, Moloni K, Kelly T, Ruoff R (2000) Strength and breaking mechanism of multiwalled carbon nanotubes under tensile load. Science 28:637–640
23. Rudawska A, Jacniacka E (2009) Analysis for determining surface free energy uncertainty by the Owen—Wendt method. Int J Adhes Adhes 29:451–457
24. Wirth CT, Hofmann S, Robertson J (2008) Surface properties of vertically aligned carbon nanotube arrays. Diam Relat Mat 17: 1518–1524
25. Ramos SC, Vasconcelos G, Antunes EF, Lobo AO, Trava-Airoldi VJ, Corat EJ (2010) Total Re-establishment of superhydrophobicity of vertically-aligned carbon nanotubes by CO_2 laser treatment. Surf Coat Tech 204:3073–3077
26. Mennella V, Monaco G, Colangeli L, Bussoletti E (1995) Raman spectra of carbon based materials. Carbon 33:115–121
27. Osswald S, Flahaut E, Ye Y, Gogotsi Y (2005) Elimination of D-band in Raman spectra of doublewall carbon nanotubes by oxidation. Chem Phys Lett 402:422–427
28. Compagnini G, Puglisi O, Foti G (1997) Raman spectra of virgin and damaged graphite edge planes. Carbon 35:1793–1797
29. Souza Filho AG, Jorio A, Samsonidze G, Dresselhaus G, Dresselhaus MS (2003) Raman spectroscopy for probing chemically/physically induced phenomena in carbon nanotubes. Nanotechnology 14:1130–1139
30. Rao AM, Jorio A, Pimenta MA, Dantas MSS, Saito R, Dresselhaus G, Dresselhaus MS (2000) Polarized Raman study of aligned multiwalled carbon nanotubes. Phys Rev Lett 84:1820–1823
31. Ya-P Sun, Fu K, Lin Y, Huang W (2002) Functionalized carbon nanotubes: properties and applications. Acc Chem Res 35: 1096–1104
32. Ueda T, Katsuki S, Abhari NH, Ikegami T, Mitsugi F, Nakamiya T (2008) Effect of laser irradiation on carbon nanotube films for Nox gas sensor. Surf Coat Tech 202:5325–5328
33. Dorai R, Kushner M (2003) A model for plasma modification of polypropylene using atmospheric pressure discharges. J Phys D Appl Phys 36:666–685
34. Boudoua JP, Martinez-Alonzo A, Tascon JM (2000) Introduction of acidic groups at the surface of activated carbon by microwave-induced oxygen plasma at low pressure. Carbon 38:1021–1029
35. Hueso JL, Espinós JP, Caballero A, Cotrino J, Gonzalez-Elipe AR (2007) XPS investigation of the reaction of carbon with NO, O_2, N_2 and H_2O plasmas. Carbon 45:89–96
36. Paredes JI, Martınez-Alonso A, Tascon JMD (2000) Atomic force microscopy investigation of the surface modification of highly oriented pyrolytic graphite by oxygen plasma. J Mater Chem 10:1585–1591
37. Estrade-Szwarckopf H (2004) XPS photoemission in carbonaceous materials: a ''Defect'' peak beside the graphitic asymmetric peak. Carbon 42:1713–1721
38. Liu M, Yang Y, Zhu T, Liu Z (2005) Chemical modification of single-walled carbon nanotubes with peroxytrifluoroacetic acid. Carbon 43:1470–1478
39. Barthlott W, Schimmel T, Wiersch S, Koch K, Brede M, Barczewski M, Kaltenmaier A, Leder A, Bohn HF (2010) The Salvinia paradox: superhydrophobic surfaces with hydrophilic pins for air retention under water. Adv Mater 22:2325–2328